Forecasting Vegetation Behavior Based on PlanetScope Time Series Data Using RNN-Based Models

Aleš Marsetič and Urška Kanjir

***Abstract*—Accurate vegetation behavior forecasting is essential for understanding the dynamics of plant life in the context of climate change and other natural or human-induced disturbances. Recurrent neural network (RNN) deep learning (DL) models represent a modern approach to predict vegetation behavior with a high level of precision. In this article, we explore the potential of different DL and more traditional methods to forecast the normalized difference vegetation index (NDVI), which is directly related to the state of vegetation and its dynamics. A time-series dataset consisting of 70 NDVI images calculated from PlanetScope data from April 2017 to January 2023 was used. Initially, all selected methods were evaluated and compared. From the six tested methods, simple RNN (SRNN) proved to be the most accurate method for predicting vegetation dynamics. The SRNN model results achieved a mean RMSE of 0.051 when compared to the actual 2022 NDVI values. The high accuracy was reflected in all five studied vegetation classes characterizing the selected Mediterranean test area. The SRNN method performs very well in most months, except in autumn where it underestimates NDVI values. To get a thorough insight into the results, we also compared them to the Sentinel-2 NDVI data and climate data consisting of temperature and precipitation values. It was found that most of the prediction differences were due to the irregular variations in meteorological conditions during the year analyzed. The predictive capabilities of RNNs are an effective tool for forecasting vegetation dynamics but can be further improved by incorporating climate data into the prediction process.**

***Index Terms*—Climatic data, deep learning (DL), normalized difference vegetation index (NDVI), satellite imagery, spatio-temporal prediction, vegetation dynamics.**

I. Introduction

In THE face of ongoing climate change and rapid human interventions, the necessity of monitoring vegetation dynamics is inevitable [1] and important for effective biodiversity management. Variations in spectral reflectance occur in vegetation phenology due to changing life cycle patterns, seasonal shifts, and prevailing weather conditions. To study the intrinsic characteristics of vegetation, it is necessary to consider the spatio-temporal dynamics of the individual units that make up the observed vegetation types.

The prediction of vegetation behavior consists of detecting the state of vegetation by observing it from the same observation point(s) over different periods and scales. In particular, the study of seasonal phenology and productivity patterns has the potential to be especially useful for identifying or forecasting such events [2]. Remote sensing technology can comprehensively detect and monitor vegetation dynamics using multitemporal remote sensing observations.

With a wide variety of satellite data available today, the analysis of time series of satellite images is currently one of the most important trends in the study of vegetation. Time series analysis has the potential to reveal long-term surface dynamics based on the temporal profile of the data for a given pixel. Time series data with higher temporal resolution provide a more accurate representation of vegetation changes, including seasonal variations, gradual shifts, and sudden, abrupt changes and are often used to evaluate smaller/shorter-term changes [3]. Vegetation indices derived from satellite data are commonly used to monitor vegetation, as they provide a high correlation with vegetation growth. Of the myriad indices used for vegetation analysis, the normalized difference vegetation index (NDVI) is the best known and most commonly used, followed by the enhanced vegetation index (EVI) and other specific vegetation-related indices used in vegetation prediction research [4], [5]. The NDVI is inversed by the ratio of near-infrared (NIR) and red (R) reflectance [6] and its values range from -1 to 1, with higher values indicating greater photosynthetic activity. Therefore, it is crucial for monitoring various global vegetation dynamics over time [7]. The continuous change in NDVI over time during plant growth provides the most intuitive information for reconstruction purposes [8]. Clouds and poor atmospheric conditions tend to lower the NDVI values [9] and cause sudden drops in the time series, which we need to remove by smoothing techniques [10].

Alterations in climatic factors have a considerable influence on vegetation dynamics, with precipitation, solar radiation, and temperature playing a central role in vegetation growth [11].

Manuscript received 6 October 2023; revised 17 January 2024; accepted 9 February 2024. Date of publication 14 February 2024; date of current version 23 February 2024. This work was supported by the Slovenian Research Agency under the Research Project J2-4488 (automatic optical satellite image orthorectification and registration with advanced deep learning methods) and Project J2-3055 (ROVI—Innovative radar and optical satellite image time series fusion and processing for monitoring the natural environment) and the Program P6-0079 (Anthropological and Spatial Studies). *(Corresponding author: Urška Kanjir.)*

Aleš Marsetič is with the Research Centre of the Slovenian Academy of Sciences and Arts, 1000 Ljubljana, Slovenia, and also with the SPACE-SI, 1000 Ljubljana, Slovenia (e-mail: ales.marsetic@zrc-sazu.si).

Urška Kanjir is with the Research Centre of the Slovenian Academy of Sciences and Arts, 1000 Ljubljana, Slovenia (e-mail: ursa.kanjir@zrc-sazu.si).

Digital Object Identifier 10.1109/JSTARS.2024.3365971

In vegetation prediction studies, the combination of NDVI and meteorological data is therefore the most commonly used dataset [5]. In the work of [12], mean precipitation in July was the most important improvement parameter for the predicting vegetation of vegetation among many environmental variables tested.

In recent years, we have observed a paradigm shift in the processing and analysis of images through the use of machine learning methods. Machine learning offers the potential for effective and efficient classification of Earth observation images. One of its main strengths lies in its ability to handle high-dimensional data and accurately define classes with very complex features [13]. In previous research, the prediction of vegetation behavior has been performed using various machine-learning techniques [5], [14], [15]. In particular, deep learning (DL), a branch of cutting-edge machine learning techniques, has gained great popularity as the method of choice for predicting vegetation patterns from image data [1], [12], [16]. This is partly due to recent developments in algorithms and increased computational resources. In addition, the ability of DL to autonomously learn and extract both linear and nonlinear hierarchical features from data, facilitated by its multilayer architecture, has played a significant role in its application for vegetation prediction [17]. DL models can provide very accurate classification results if they have sufficiently large data sets and appropriate labeling. Therefore, good reference (training) data is of great importance when dealing with DL.

A widely used framework in the field of DL is a recurrent neural network (RNN), which has been used for vegetation monitoring and prediction for nearly a decade [18], [19], [20], [21]. RNNs are well suited for tasks that require sequences, such as time series prediction, natural language processing, machine translation, voice recognition, image labeling, and others, as they are capable of processing inputs of varying lengths [22]. Unlike other deep networks, such as convolutional neural networks, which typically lack connections between neurons within the same layer, the RNN contains feedback loops in its hidden layer to capture sequential information in the data [23], such as satellite time series, to perform classification or prediction. RNNs have the ability to use the information of previous inputs to generate the following outputs of the sequence. This is done by feeding the results of a particular layer back into the input layer to predict the output. But at the same time, the computation can be very slow and struggle with the problem of vanishing gradient. This problem occurs when the gradients used to calculate the weight updates approach values close to zero, making the network unable to acquire new weight information. This problem becomes more pronounced as the depth of the network increases. Therefore, a DL model has been developed that effectively addresses the vanishing gradient issue, called long short-term memory (LSTM) [24]. It has similarities with a conventional RNN but differs in that each standard node in the hidden layer is replaced by a memory cell [22]. The most important feature of the LSTM is its cell state, which has the ability to store information over large time intervals. This attribute enhances the model's efficacy in preserving long-term patterns in data sequences [18]. In addition, the LSTM is superior to the conventional RNN because it is better able to address the problems that arise in backpropagation through time (BPTT). In addition to a lower probability of experiencing vanishing gradients, it also includes a "gradient clipping" method to prevent explosive gradients during BPTT [18]. To predict vegetation dynamics over large areas, [1] implemented an LSTM model using moderate resolution imaging spectroradiometer (MODIS) NDVI time series data and achieved high accuracy. More recently, Ahmad et al. [18] used an optimized convolutional LSTM to make NDVI predictions for soybean at multipixel field level, also using MODIS time series data. The same type of dataset and LSTM model was used to forecast vegetation health in Kenya [25] and to predict Mediterranean vegetation on the Greek island of Lesbos [26]. All mentioned authors found that LSTM provides sufficiently accurate forecasts, especially in the context of drought monitoring and vegetation forecasting. These results emphasize the superior performance of LSTM compared to a shallower neural network.

Another approach that effectively addresses the problem of the vanishing gradient inherent in a standard RNN is the gated recurrent unit (GRU) method [27], which can also handle multivariate time series image data. Compared to LSTM, GRU is characterized by a smaller number of parameters and a relatively simpler training process. Numerous researchers have performed comparisons between GRU and LSTM [21], [28], [29], and their findings consistently indicate that GRU can achieve equivalent or even better learning outcomes than LSTM in various applications. For example, in plant disease detection and prediction, it has been shown to perform well when time series data are included [30]. Zhang et al. [31] showed that the GRU-based vegetation model has a high degree of accuracy in simulating vegetation dynamics in arid and semi-arid regions. In addition, the model proved to be adept at recognizing the temporal characteristics of dynamic data by integrating static information holistically. The findings of [32] also show that the GRU model is a viable solution for predicting forest phenology. It not only provides valuable insights into future forest growth but also lays the foundation for the practical application of forest phenological prediction. However, it should be noted that GRU as a variant of RNN has its limitations. It focuses primarily on retaining sequential information but does not examine the significance of individual elements within sequences, and learning GRU is very difficult for long sequences [33]. Nevertheless, GRU has emerged as the preferred method for phenological prediction due to its simple internal structure and relatively short training time, as pointed out in [32].

This study addresses the performance of six different vegetation prediction methods: three RNNs [a Simple RNN (SRNN), an LSTM and a GRU DL model], a simple 1D convolution (Conv1D), and two more traditional methods [random forest (RF) and autoregressive integrated moving average (ARIMA)] using very high-resolution PlanetScope time series images between the years 2017 and 2023. PlanetScope satellites have the ability to observe the Earth's surface with a high combination of temporal and spatial resolution and have rarely been used for vegetation prediction. For our study, we evaluated the suitability of the six mentioned models for vegetation prediction in a Mediterranean area in Slovenia. We also evaluated the model

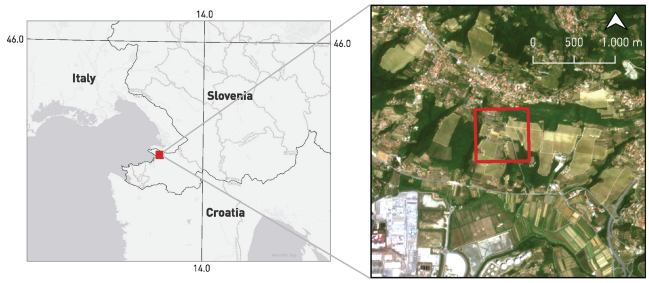

Fig. 1. Study area is located in the south-western part of Slovenia. The small test subset is marked with a red square.

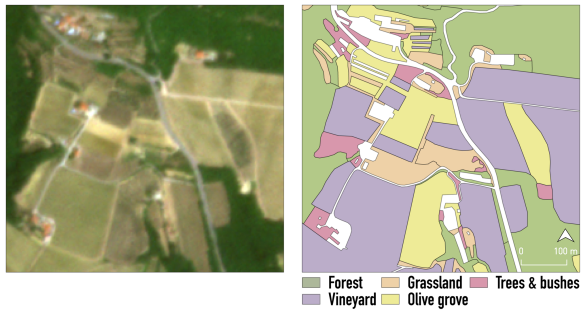

Fig. 2. Original PlanetScope satellite image taken on July 15th, 2022 (left) and the vegetation classes contained in the reference data (right).

predictions obtained from the PlanetScope images, by comparing them with Sentinel-2 images and climate data (temperature and precipitation), which served as proxies for climate patterns, as these variables are directly related to vegetation activity.

The goals of this article are as follows.

1) To develop and evaluate DL and more traditional models using high spatio-temporal resolution PlanetScope time series data.
2) To identify and predict the behavior of five different vegetation classes in a Mediterranean area for the year 2022.
3) To correlate the results with other satellite data (Sentinel-2) and climate data (temperature, precipitation).

The structure of this article is outlined as follows. Section II provides an insight into the area of investigation, the materials used for the task, and the methods used for model training and testing. This section also provides a detailed explanation of the RNN model. In Section III, we present the results of our models, perform an evaluation, and compare them with the Sentinel-2 time series data. We also compare findings with the climate data. Section IV is dedicated to a comprehensive discussion of the results obtained. Finally, in Section V, we highlight possible future trends that should be investigated.

II. Data and Methods

A. Study Area and Data

We performed the analysis in the coastal region in the south-western part of Slovenia (see Fig. 1). The region is relatively flat, which means that the satellite images are not affected by shadows caused by the terrain. The climate is Mediterranean, characterized by an average annual temperature of 14.4 °C and an average annual precipitation of 1056 mm per year. The vegetation types in the area include five main classes of land use/land cover (LULC): forest, grassland, vineyards, olive groves, and trees and bushes. To manage the computational complexity of the models, our study focused on a smaller test area of 600 × 600 m (40 000 PlanetScope image pixels). More than 70% of the test area is covered by the five observed vegetation types.

1) Satellite Data: In this study, we used commercially available PlanetScope images with a spatial resolution of 3 m obtained from the Planet data service platform [34]. PlanetScope provides near-daily images of the Earth's surface, which is particularly useful for areas that are frequently covered by clouds.

TABLE I
LULC Classes Defined in Our Study Area in Percent and by Number of Pixels

Land cover type	area percentage	number of pixels
Forest	26.8%	7739
Grassland	6.9%	2006
Vineyard	44.6%	12913
Olive grove	18.0%	5198
Trees and bushes	3.7%	1067

The data includes four reflectance bands (blue, green, red, and NIR). We downloaded Level 3B PlanetScope images, meaning that the images were already orthorectified and included geometric, radiometric, and atmospheric corrections [35]. The datasets were acquired in geo-tiff format and projected to UTM Zone 33N on the WGS 84 ellipsoid. We constructed a time series from April 2017 to January 2023, limiting to a single noncloudy image per month. We calculated the NDVI for all 70 noncloudy images. To compare the calculated results, we also used Sentinel-2 NDVI data for the year 2022, which we obtained from the SentinelHub repository [36].

2) In-Situ Data: The reference data used in the study for training and validation are derived from the actual land use data layer. These are vector formatted data from the Register of Actual Agricultural and Forestry Land Use (RABA), which is managed and maintained by the Ministry of Agriculture, Forestry and Food of the Republic of Slovenia. We used freely available data from 2020 downloaded from the Ministry's website [37]. The data were cleaned to reduce false detections, and the reference data were grouped into meaningful and most frequent LULC classes according to their closest similarity. In addition, some rare labels were merged into one of the five classes of interest. We also set the minimum size of the areas that could still be meaningfully identified in the analyzed Planet data to 100 m^2.

We applied an inner buffer of one pixel to all polygons to avoid erroneous calculations at the boundaries of the polygons. The original satellite image and the distribution of vegetation class labels over our study area are shown in Fig. 2. Table I shows the

Fig. 3. Workflow of the proposed methodology.

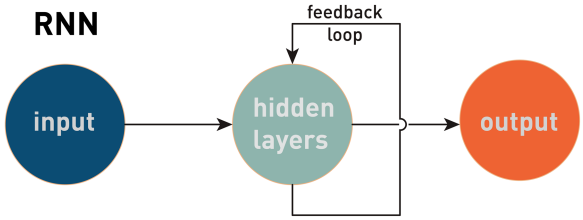

Fig. 4. General structure of an SRNN network with an input, hidden layers, output, and feedback loop.

proportion of LULC classes (forest, grassland, vineyard, olive grove, and trees and bushes) used for the study.

3) Climatic Data: The monthly data set for total precipitation (mm) and average temperature (°C) for our study area for the period 2017–2023 was obtained from the Slovenian Environment Agency (ARSO meteorological data archive). As temperature and precipitation are important factors that directly affect vegetation cycles, the dataset was used to compare with the results obtained from satellite data to correlate and contextualize the predicted results.

B. Methodology

The workflow consists of three basic steps: data preparation, RNN training, and validation, where the first step is composed of several substeps (see Fig. 3).

1) Data Preparation: To process the data more efficiently, we have converted the time series into long sequences of a tabular format data. This way, each pixel has its own row with information about the band values, the NDVI, the *X*- and *Y*-coordinates, the acquisition date and the vegetation type labeling, which we obtained from the RABA layer. After formatting the data of the complete time series in the same way, they were saved in a parquet file. This file was then used to test the method.

Before using the input time series data in the neural networks, we implemented a Savitzky-Golay temporal filter [38] on the time series. The best fit was achieved with a 7th-degree polynomial on a window of size 11.

2) RNN Training: The general structure of an RNN consists of an input layer, various hidden and dense layers and the output layer (see Fig. 4). The most important feature is the feedback loop, which allows the RNN to "memorize" the information during training.

The input layer takes the input data into the neural network and then forwards it to the middle part, which usually consists of several hidden layers, each with its own activation function, weights, and biases. These are standardized so that each hidden layer has the same parameters in all time steps. This reduces the number of parameters to be learned and can lead to better generalization. Instead of several hidden layers, a single hidden layer is then created and run through as often as necessary in a loop.

The RNN handles the input sequence by using a recurrent hidden state, where the activation at each time step relies on the previous time step's activation, resulting in dynamic temporal behavior [39].

Given a sequence $x = (x_1, x_2, \ldots, x_i)$, where x_i is the data at the ith time step, the update of the recurrent hidden state h_t is implemented as follows:

$$h_t = f\left(Wx_t + Uh_{t-1} + b_h\right). \tag{1}$$

In this context, the equation involves the use of a nonlinear activation function, referred to as f, which is typically chosen from a linear activation function (usually sigmoid, tangent, or rectified linear unit—ReLU). W and U represent the weights associated with the inputs and hidden units in the recurrent layer, and b_h represents the bias associated with the recurrent layer. The output y at time t is calculated as

$$y_t = f\left(Vh_t + b_y\right) \tag{2}$$

where V are the weights associated with the hidden units to the output units, and b_y is the bias associated with the feedforward layer.

Different types of RNNs can be used to predict data. The simplest is the SRNN, while the LSTM uses memory cells that are capable to store information for extended durations, regulated by a set of gates. GRU, on the other hand, uses a smaller set of gates without separate memory cells, representing a somewhat less intricate architecture. In our study, an SRNN with two blocks of 50 hidden units, one dense unit and a sequence length of 10 was used to process time series. The activation function was ReLU and the Adam optimizer was used in the network.

The prediction was made separately for each pixel based on the time sequence. Before processing, the input time series data was split into two subsets that were used for training and testing (validation). The testing subset helps to evaluate the neural network's performance when applied to new data. Since we had 70 time steps, 47 time steps (67.1% of the data) were used for training and 23 time steps (32.9%) for testing. This left enough data to predict the next 12 forecast steps (12 months of 2022). Moreover, studies have shown that a 70:30 split of the data results in a more robust evaluation of the network [20].

3) Validation: The validation was divided into two parts. The first part analyzed the generated forecast NDVI rasters and compared them with the NDVI calculated from the actual PlanetScope images for the year 2022. In the second part, the forecasted NDVI was compared with the actual Sentinel-2-based NDVI data and the climatic (meteorological) data.

III. Results

Before analyzing the results obtained, the reasons for choosing SRNN as the main method for conducting the experiments are outlined and explained. This is followed by an evaluation of the data predicted by SRNN compared to the actual data. In the last part, the predictions for PlanetScope satellite data are

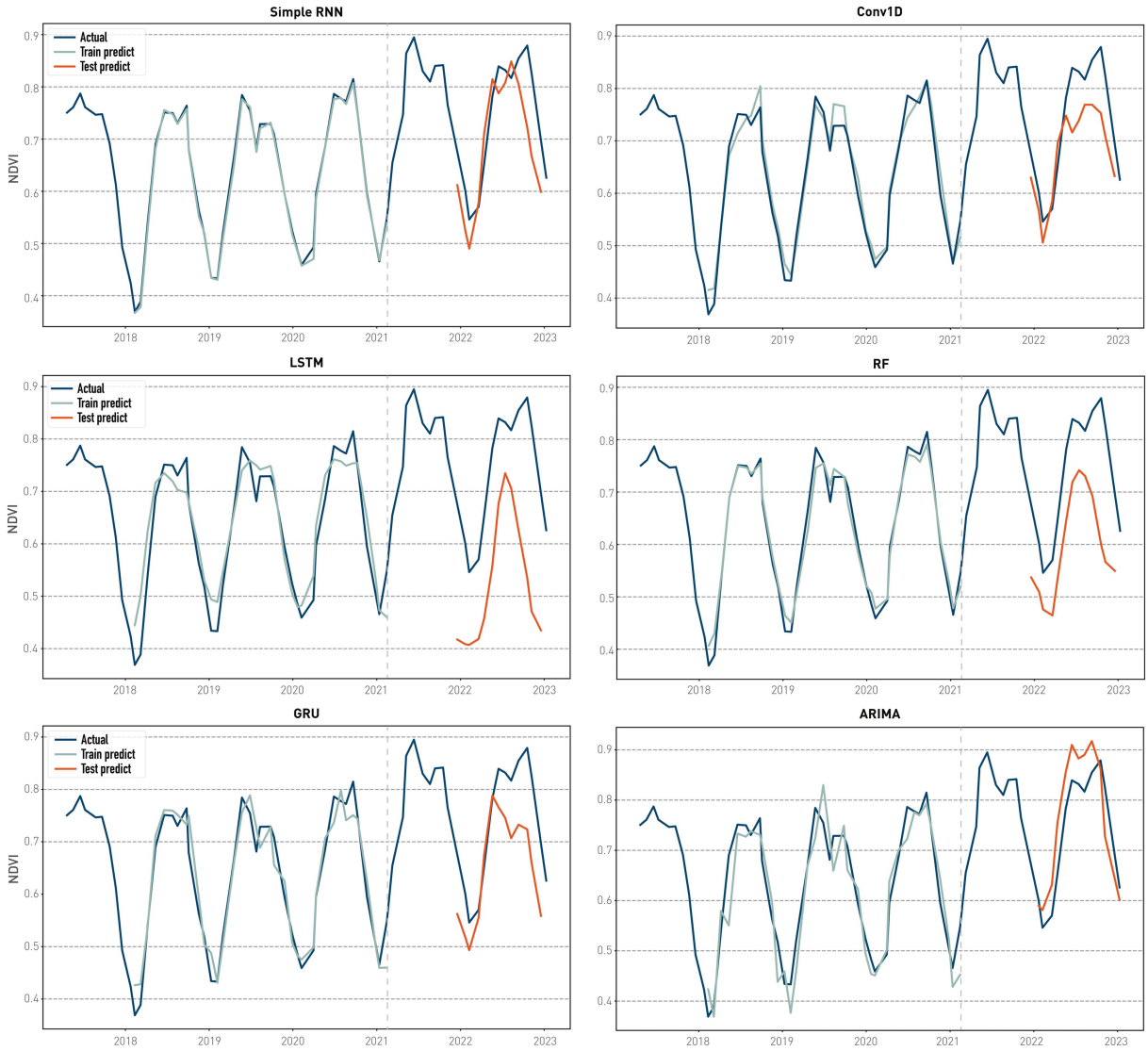

Fig. 5. Comparison among SRNN, LSTM, GRU, Conv1D, RF, and ARIMA models for a single typical forest pixel. The dashed line represents the separation between the training (left) and test (right) data.

analyzed in comparison to the Sentinel-2 data and the behavior of the time series data using external climate data is explained.

A. Comparison With Other RNN Methods

We used the SRNN network to predict the NDVI values in the area we selected. This decision was based on the results we obtained in predicting the NDVI on various pixels from five different LULC classes using various machine-learning methods and DL networks. Besides the three RNN networks (SRNN, LSTM, and GRU) we also tested a simple convolution method—Conv1D. Conv1D can be used for forecasting and is suitable for processing one-dimensional sequences, such as time series data, as it operates on a single spatial dimension. It is also faster than the RNN networks. All four DL networks mentioned were implemented with the same number of layers.

In addition, we tested two traditional models, which are still widely used. The RF algorithm [40] has proven to be extremely successful as a general-purpose classification and regression method. The approach, which combines multiple random decision trees, has shown excellent performance on a large number of variables. The other model is the ARIMA, which is very popular for forecasting time series [41]. In the processing, we used the upgraded model called SARIMAX, which describes the seasonality and relations within the time series in a more complex way.

Table II shows the comparative accuracies of the models tested. The RMSEs obtained are the mean values of all RMSEs calculated for each vegetation pixel in the test area.

Both the numbers and the visual representation (Fig. 5) show that the SRNN achieved better results in our study than the other methods. It accurately predicts the training data with an average RMSE of 0.012 and is very good at predicting the NDVI data with an RMSE of 0.051. The second-best result was obtained with Conv1D, which was surprisingly close to the SRNN in terms of accuracy and processing time. The results obtained with

TABLE II
COMPARISON BETWEEN ACCURACIES OBTAINED WITH SRNN, LSTM, GRU, CONV1D, RF, AND ARIMA

Method	RMSE train	RMSE test
SRNN	0.012	0.051
LSTM	0.032	0.093
GRU	0.025	0.065
Conv1D	0.013	0.053
RF	0.015	0.084
ARIMA	0.039	0.088

GRU are similar but slightly worse. The worst results on the test data were achieved by LSTM, closely followed by the ARIMA and RF methods. The average RMSE of the LSTM for the predicted data is almost twice as large. The RF regressor appears to have overfitted the train data, as the difference between train and test RMSE was the largest. The poor results of ARIMA can be attributed to the relatively short time series (small number of observations) that led to occasional bad directions in the line search and failed convergences.

B. Training and Accuracy Assessment

Next, we compared the predictions of the SRNN with the actual NDVI data and analyzed them in more detail. The trained neural network generated estimations for 12 time steps corresponding to all 12 months of the year 2022. These were compared with the actual NDVI data calculated from satellite images. The comparison provided valuable insights into both the distribution of NDVI values and the performance of the RNN network. Table III shows the monthly similarities and differences between the predicted and actual NDVI values for all vegetation pixels. The Pearson correlation coefficient (R), calculated from all vegetation pixels within the test area, is significantly higher from May to September, while the correlation is poorest in November. As will be explained in Section III-C, the main reason for these differences is directly related to the exceptional weather in the observed year.

The other calculated parameter is the RMSE, which is also calculated from all vegetation pixels within the test area and shows significantly higher values from October to December. The RMSE values are in general in line with the correlation coefficient, however, they do not vary much from January to September.

The same behavior can be observed in the monthly scatter plots in Fig. 6. The correlation between predicted and actual NDVI is very high in the summer months (over 0.95), while the lowest correlation is found in the winter months (about 0.8).

Similar results, characterized by stronger correlations during the summer months and weaker ones during the winter months,

TABLE III
COMPARISON BETWEEN PREDICTED AND ACTUAL NDVI MEASURED BY PEARSON CORR. COEFFICIENT AND RMSE

Month	Pearson corr. coefficient (R)	RMSE
January	0.85	0.056
February	0.82	0.052
March	0.88	0.079
April	0.86	0.083
May	0.92	0.055
June	0.96	0.052
July	0.97	0.043
August	0.96	0.051
September	0.92	0.055
October	0.82	0.086
November	0.77	0.135
December	0.86	0.118

have been reported in previous studies using other satellite time series data sources, as can be seen in studies such as [1] or [26].

In addition to the monthly comparison for all pixels, we also compared the predicted and actual NDVI for each vegetation class. The results are presented in Fig. 7. The predicted values show the expected behavior of the vegetation with two main peaks at the beginning and in the second part of the summer, with a small drop in dry July. On the other hand, the actual NDVI values show an unusual pattern with the highest values in October or November.

Of all classes, the forest class has the highest NDVI during most of the year, as expected. For all classes, the two values (predicted and actual) are very similar in the first part of the year, but they differ in the second part of the year—the actual values are higher.

Fig. 8 shows a spatial comparison illustrating the similarity between the predicted and actual NDVI values for the 12 predicted months. The images reveal a high degree of consistency between the actual and predicted NDVI values. The differences are predominantly within 0.1 (yellow and light green) for most of the study area for the entire year 2022, while higher differences were found in some patches in March and April and especially from October to December. These exceptions correlate strongly with the RMSEs achieved (see Table III). In these months, the differences are highest in the forest patches and some vineyard

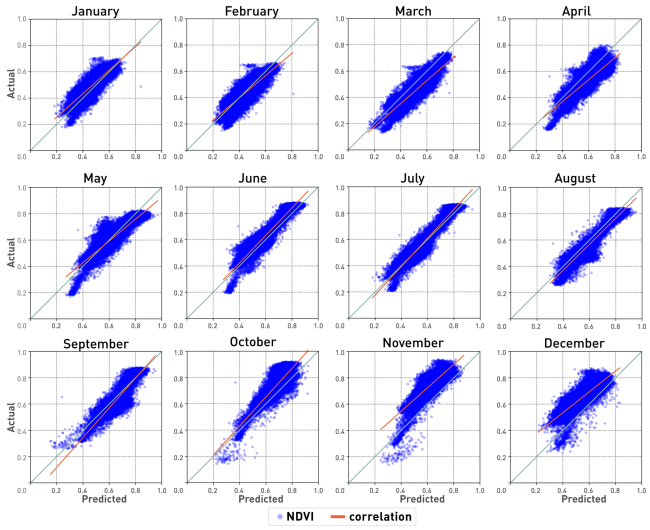

Fig. 6. Scatterplots for each month of the year 2022. On each scatterplot, the x-axis shows the predicted NDVI values and the y-axis the actual NDVI values.

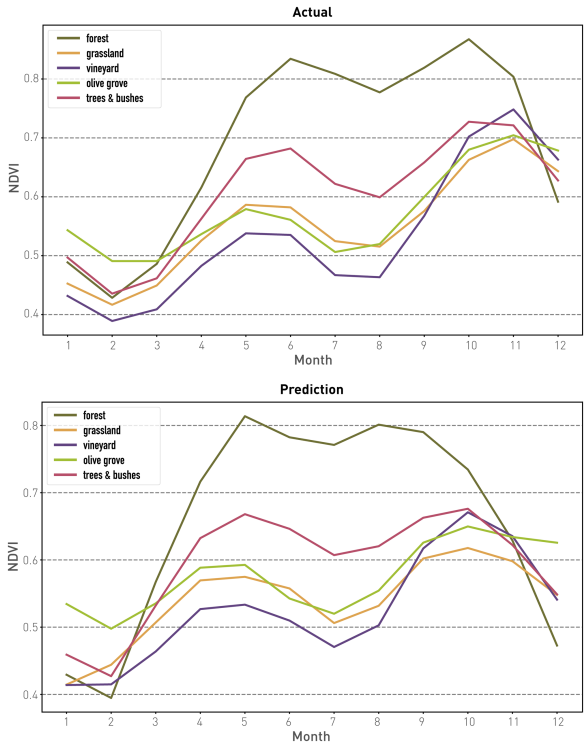

Fig. 7. Actual and predicted NDVI values obtained from PlanetScope data for each class.

patches. One possible reason for this could be the variability of temperature and precipitation between the training and test years, which is analyzed in Section III-C.

C. Comparison With Sentinel-2 and Climatic Data

As mentioned in Section II-A, we calculated the NDVI from the Sentinel-2 images of the year 2022 to obtain additional validation data for our model. We compared these values with the actual PlanetScope NDVI values and the NDVI values predicted by SRNN for each of the five vegetation classes (see Fig. 9). In addition, Fig. 10 shows the actual Sentinel-2 NDVI values for each of the five vegetation classes together for each month of 2022.

TABLE IV
CORRELATION BETWEEN PREDICTED PLANET DATA AND ACTUAL SENTINEL-2 DATA

Vegetation class	Pearson corr. coefficient (R)	RMSE
Forest	0.84	0.102
Grassland	0.70	0.067
Vineyard	0.78	0.081
Olive grove	0.77	0.060
Trees and bushes	0.69	0.064

As shown in Fig. 9, the NDVI values calculated from both satellite data show similar values, except in July and August, when the Sentinel-2 values are lower for all classes except for forest class. When performing a correlation test, the analysis showed a significant correlation between the predicted Planet data values and the Sentinel-2 data for all vegetation classes (see Table IV). The best correlation is for the forest class ($R = 0.84$) and the worst for the trees and bushes class ($R = 0.69$). On the other hand, the forest RMSE shows a more scattered distribution.

We also examined the main climate parameters at the time of our observation. Fig. 11 shows the average temperature and precipitation for 2017–2021 as lines, while both climate data for 2022 are shown as bars. September 2022 was extremely wet (blue bar), preceded by four very hot and dry months (drier than average). This could explain the high actual NDVI values in autumn 2022, which led to a lower accuracy of the SRNN model predictions. This finding suggests that meteorological data should be added to the SRNN to enable a more accurate forecast.

IV. DISCUSSION

The main objective of this study was to investigate the performance of RNN models when applied to very high-resolution data for the prediction of NDVI for different vegetation types. As observed in numerous previous studies [35], training RNNs to capture extended temporal dependencies can be challenging due to the tendency of gradients to vanish. This is the result of variations in gradient magnitudes and the fact that short-term dependencies predominate over long-term dependencies. This is especially true for long time-series data, as the long-term dependencies become exponentially smaller with increasing sequence length [39].

However, our PlanetScope dataset was relatively short. When the sequence length is shorter, it is advisable to compare different RNN architectures and to choose a simpler one—which is, if not

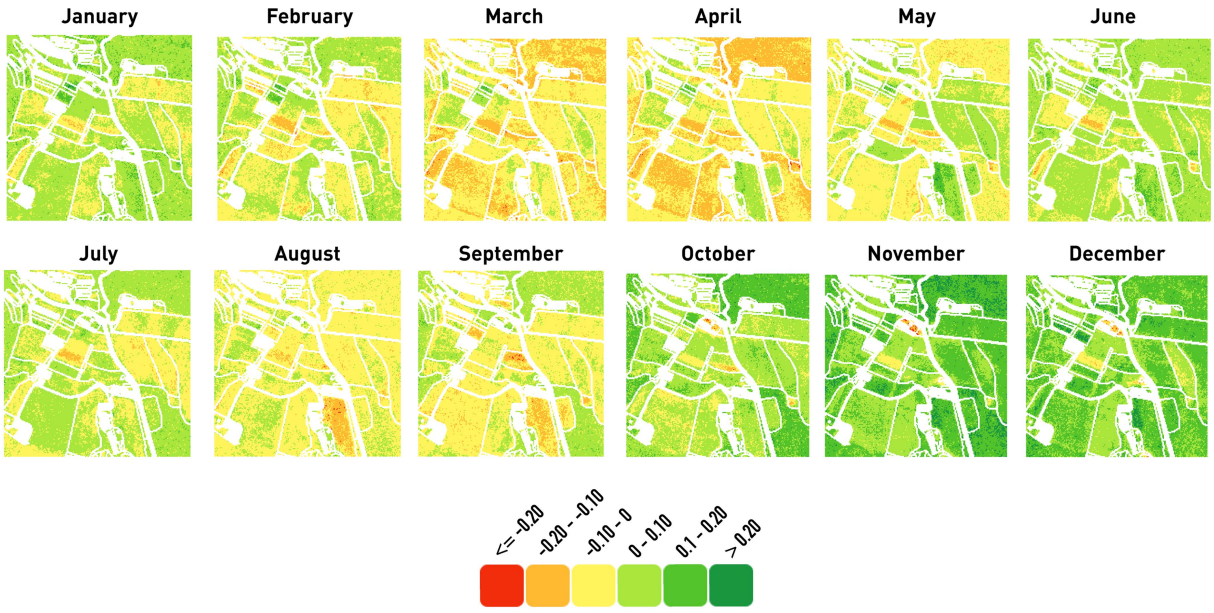

Fig. 8. Spatial distribution of the differences between the forecasted and actual NDVI per month on the study area.

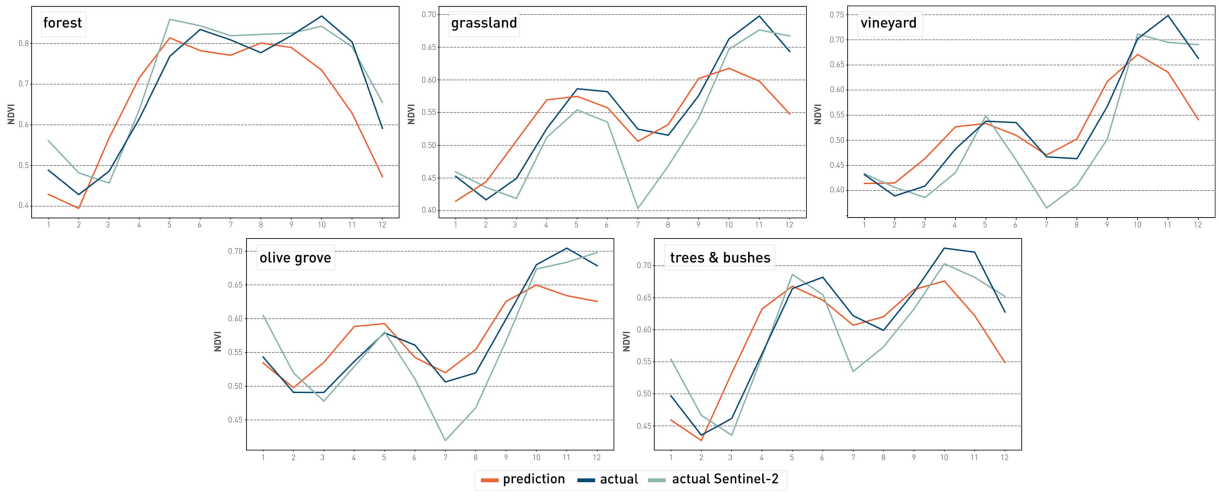

Fig. 9. Comparison of the actual Sentinel-2 NDVI and the actual and predicted PlanetScope NDVI for each vegetation class in the year 2022.

much better, at least faster. This was the main reason why we initially tested different RNN approaches to predict vegetation behavior with a high level of precision. At the same time, however, we were acknowledged by the fact that deep neural networks generally perform worse than traditional models on small datasets [43]. In contrast to this finding, SRNNs in our case still performed better than RF or even ARIMA, which are among the best non-DL methods for time series forecasting.

Throughout the study, the same number of hidden layers was used in each of the neural network models analyzed in order to improve the comparability of the results. According to empirical tests in which we used different configurations (number of layers and their size), two hidden layers seemed to be the best architecture for GRU and LSTM, while for SRNN a single hidden layer gave slightly better results. Nevertheless, the results do not differ significantly between the different configurations of the chosen model.

In the case of SRNN, high accuracy was achieved for all five different Mediterranean vegetation classes analyzed for each month. However, it was found that the results are not always consistent within the class: in some patches, the difference between the predictions and the actual values is substantially higher than in others. This is particularly true for the vineyards class, especially for the southernmost central plot (see Fig. 8). It turned out that the patch in question had only recently been planted with young vines, so the reflectance is composed of the barren soil, the young vines and the grass growing between them. Another anomaly was observed on a grassland patch where the land use had been changed from grassland to arable land for vegetable cultivation.

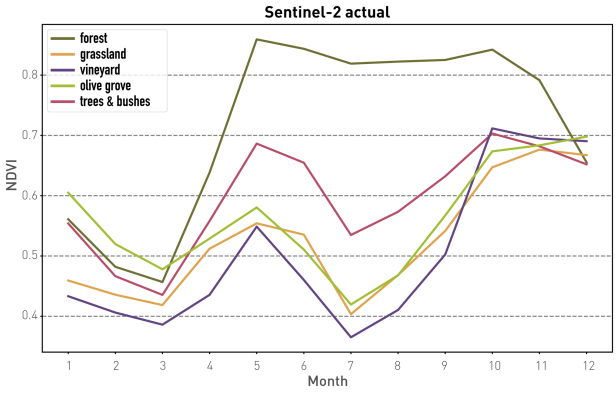

Fig. 10. Actual NDVI from Sentinel-2 for each vegetation class.

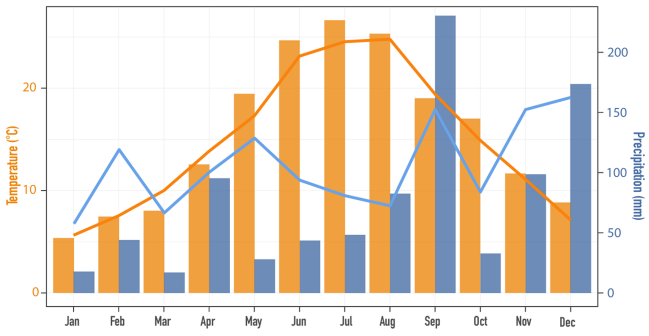

Fig. 11. Comparison of the monthly precipitation (blue bars) and temperature (yellow bars) for 2022 with the average precipitation (light blue line) and average temperature (dark orange line) for 2017–2021.

Furthermore, the findings indicate that the SRNN method exhibits superior performance during the summer months (e.g., the correlation in July is 0.97), while the correlation between the actual and predicted NDVI values drops to 0.77 in the autumn months (from October to December). To thoroughly analyze the results, they were compared with the Sentinel-2 NDVI data and climate data consisting of temperature and precipitation values. The main difference between the two sensors lies in the fact that PlanetScope images offer a higher temporal and spatial resolution compared to the Sentinel-2 data, but a lower radiometric resolution. Nevertheless, the PlanetScope data are characterized by the fact that they recognize finer details on the field scale [4]. A comparison of the predictions with the actual data revealed that the Sentinel-2 data gave an average correlation of 0.76 and performed similarly well to the Planet data in the summer months while underestimating the NDVI in the autumn months. The climate data revealed the cause of these discrepancies—an extremely wet September after very dry summer months, which led to above-average NDVI values in the autumn months. As already observed in other studies [12], we conclude here that the predictive capabilities of RNNs are an effective tool for forecasting vegetation dynamics, but can be further improved by incorporating climate data into the forecasting process.

The NDVI forecasting was performed on the basis of individual pixels. As a result, the resulting images look grainy and discontinuous in some regions. To avoid this granularity, a more complex architecture is required that also takes into account the neighboring pixels. Some studies have already been conducted using convolutional RNN-based DL architectures [18], but they have not been extensively tested on different types of data.

To summarize, the procedure performed well in a Mediterranean area in Slovenia. Further tests in other geographical regions and other ecosystems are needed to gain a better understanding of the performance of the architecture used. It should be noted that the study area was relatively flat and the reflectance values were not affected by shadows. Predictions in more hilly terrain could be difficult, especially when trying to analyze values belonging to the same vegetation class but under different illumination conditions. For the same reason, it would be difficult to train a model on flat terrain and then use it to predict vegetation dynamics in areas with complex illumination.

V. Conclusion

In this work, we performed an evaluation and comparison of different approaches for the qualitative prediction of vegetation dynamics using a relatively short time series of PlanetScope data. These approaches included three RNNs (SRNN, a LSTM, and a GRU), a Conv1D and two more traditional methods (RF and ARIMA). Our dataset comprised 70 monthly PlanetScope images, from which we derived NDVI values, spanning from April 2017 to January 2023. Our experimental findings revealed that in cases where short time series data and a limited number of parameters are employed, the SRNN exhibited superior performance compared to the other RNN methods. In particular, SRNN performed better in terms of convergence rate, processing time, and overall prediction accuracy. Conv1D was surprisingly close to SRNN in terms of accuracy and processing time, while the traditional methods performed poorly, despite achieving the fastest processing times. The poorer performance of LSTM, GRU, and ARIMA can mainly be attributed to the relatively short time series. The results obtained with the Sentinel-2 data show comparable trends. However, the almost daily access to Planet data could provide the opportunity to improve the forecast accuracy and promote digital vegetation modeling [44].

The use of climate data for vegetation prediction in RNN models is of utmost importance, as these environmental factors directly influence the vegetation greenness. In our analysis, there were some discrepancies in the predictions, especially in the autumn months. Therefore, we included climate data (temperature and precipitation) to understand the inconsistencies. It turned out that most of the discrepancies in the predictions were due to the irregular meteorological conditions in the analyzed year. For this reason, we emphasize that vegetation forecasting models should incorporate meteorological data to produce more accurate predictions. However, our results show that DL methods are a suitable tool for forecasting vegetation behavior when high-resolution time series of satellite data are used.

Acknowledgment

The authors would like to express their gratitude to Planet for providing the data as part of the Planet's Education and Research

program. In addition, the authors extend their appreciation to P. Pehani for his insightful comments on the initial draft of this article.

REFERENCES

[1] D. S. Reddy and P. R. C. Prasad, "Prediction of vegetation dynamics using NDVI time series data and LSTM," *Model. Earth Syst. Environ.*, vol. 4, no. 1, pp. 409–419, Apr. 2018, doi: 10.1007/s40808-018-0431-3.

[2] J. E. Davison, D. D. Breshears, W. J. D. van Leeuwen, and G. M. Casady, "Remotely sensed vegetation phenology and productivity along a climatic gradient: On the value of incorporating the dimension of woody plant cover," *Glob. Ecol. Biogeography*, vol. 20, no. 1, pp. 101–113, 2011, doi: 10.1111/j.1466-8238.2010.00571.x.

[3] J. Verbesselt, R. Hyndman, G. Newnham, and D. Culvenor, "Detecting trend and seasonal changes in satellite image time series," *Remote Sens. Environ.*, vol. 114, no. 1, pp. 106–115, Jan. 2010, doi: 10.1016/j.rse.2009.08.014.

[4] N. Farmonov et al., "Combining PlanetScope and Sentinel-2 images with environmental data for improved wheat yield estimation," *Int. J. Digit. Earth*, vol. 16, no. 1, pp. 847–867, Dec. 2023, doi: 10.1080/17538947.2023.2186505.

[5] A. Ferchichi, A. B. Abbes, V. Barra, and I. R. Farah, "Forecasting vegetation indices from spatio-temporal remotely sensed data using deep learning-based approaches: A systematic literature review," *Ecological Inform.*, vol. 68, May 2022, Art. no. 101552, doi: 10.1016/j.ecoinf.2022.101552.

[6] C. J. Tucker, "Red and photographic infrared linear combinations for monitoring vegetation," *Remote Sens. Environ.*, vol. 8, no. 2, pp. 127–150, May 1979, doi: 10.1016/0034-4257(79)90013-0.

[7] Z. Zhu et al., "Greening of the Earth and its drivers," *Nature Climate Change*, vol. 6, no. 8, pp. 791–795, Aug. 2016, doi: 10.1038/nclimate3004.

[8] S. Li, L. Xu, Y. Jing, H. Yin, X. Li, and X. Guan, "High-quality vegetation index product generation: A review of NDVI time series reconstruction techniques," *Int. J. Appl. Earth Observ. Geoinf.*, vol. 105, Dec. 2021, Art. no. 102640, doi: 10.1016/j.jag.2021.102640.

[9] J. Chen, P. Jönsson, M. Tamura, Z. Gu, B. Matsushita, and L. Eklundh, "A simple method for reconstructing a high-quality NDVI time-series data set based on the Savitzky–Golay filter," *Remote Sens. Environ.*, vol. 91, no. 3, pp. 332–344, Jun. 2004, doi: 10.1016/j.rse.2004.03.014.

[10] N. Pettorelli, *The Normalized Difference Vegetation Index*. London, U.K.: Oxford Univ. Press, 2013.

[11] G. Churkina and S. W. Running, "Contrasting climatic controls on the estimated productivity of global terrestrial biomes," *Ecosystems*, vol. 1, no. 2, pp. 206–215, Mar. 1998, doi: 10.1007/s100219900016.

[12] Y. Ma et al., "Forecasting vegetation dynamics in an open ecosystem by integrating deep learning and environmental variables," *Int. J. Appl. Earth Observ. Geoinf.*, vol. 114, Nov. 2022, Art. no. 103060, doi: 10.1016/j.jag.2022.103060.

[13] A. E. Maxwell, T. A. Warner, and F. Fang, "Implementation of machine-learning classification in remote sensing: An applied review," *Int. J. Remote Sens.*, vol. 39, no. 9, pp. 2784–2817, 2018, doi: 10.1080/01431161.2018.1433343.

[14] T. Kattenborn, J. Leitloff, F. Schiefer, and S. Hinz, "Review on convolutional neural networks (CNN) in vegetation remote sensing," *Int. Soc. Photogrammetry Remote Sens. J. Photogrammetry Remote Sens.*, vol. 173, pp. 24–49, Mar. 2021, doi: 10.1016/j.isprsjprs.2020.12.010.

[15] Q. Yuan et al., "Deep learning in environmental remote sensing: Achievements and challenges," *Remote Sens. Environ.*, vol. 241, May 2020, Art. no. 111716, doi: 10.1016/j.rse.2020.111716.

[16] C. Yu and B. Liu, "Context-to-image CNN approach to predict soybean yields in illinois and rural areas," 2021. Accessed: Jul. 28, 2023. [Online]. Available: https://www.semanticscholar.org/paper/Context-to-Image-CNN-Approach-to-Predict-Soybean-in-Yu/fce26d2938607e9e029c5e0db7144b0a9e08b34c

[17] V. Sagan et al., "Field-scale crop yield prediction using multi-temporal WorldView-3 and PlanetScope satellite data and deep learning," *Int. Soc. Photogrammetry Remote Sens. J. Photogrammetry Remote Sens.*, vol. 174, pp. 265–281, Apr. 2021, doi: 10.1016/j.isprsjprs.2021.02.008.

[18] R. Ahmad, B. Yang, G. Ettlin, A. Berger, and P. Rodríguez-Bocca, "A machine-learning based ConvLSTM architecture for NDVI forecasting," *Int. Trans. Oper. Res.*, vol. 30, no. 4, pp. 2025–2048, 2023, doi: 10.1111/itor.12887.

[19] L. Mou, P. Ghamisi, and X. X. Zhu, "Deep recurrent neural networks for hyperspectral image classification," *IEEE Trans. Geosci. Remote Sens.*, vol. 55, no. 7, pp. 3639–3655, Jul. 2017, doi: 10.1109/TGRS.2016.2636241.

[20] A. Stepčenko, "NDVI index forecasting using a layer recurrent neural network coupled with stepwise regression and the PCA," in *Proc. Int. Conf. Transl., Interpreting, Cogn., 5th Virtual Int. Conf. Inform. Manage. Sci.*, 2016, vol. 5, pp. 130–135.

[21] W. Yu et al., "Spatial–temporal prediction of vegetation index with deep recurrent neural networks," *IEEE Geosci. Remote Sens. Lett.*, vol. 19, 2022, Art. no. 2501105, doi: 10.1109/LGRS.2021.3064814.

[22] Z. C. Lipton, J. Berkowitz, and C. Elkan, "A critical review of recurrent neural networks for sequence learning," Jun. 2015, *arXiv:1506.00019*, doi: 10.48550/arXiv.1506.00019.

[23] F. Grisoni, M. Moret, R. Lingwood, and G. Schneider, "Bidirectional molecule generation with recurrent neural networks," *J. Chem. Inf. Model.*, vol. 60, no. 3, pp. 1175–1183, Mar. 2020, doi: 10.1021/acs.jcim.9b00943.

[24] S. Hochreiter and J. Schmidhuber, "Long short-term memory," *Neural Comput.*, vol. 9, no. 8, pp. 1735–1780, Nov. 1997, doi: 10.1162/neco.1997.9.8.1735.

[25] T. Lees, G. Tseng, C. Atzberger, S. Reece, and S. Dadson, "Deep learning for vegetation health forecasting: A case study in Kenya," *Remote Sens.*, vol. 14, no. 3, p. 698, Jan. 2022, doi: 10.3390/rs14030698.

[26] C. Vasilakos, G. E. Tsekouras, and D. Kavroudakis, "LSTM-based prediction of Mediterranean vegetation dynamics using NDVI time-series data," *Land*, vol. 11, no. 6, p. 923, Jun. 2022, doi: 10.3390/land11060923.

[27] K. Cho, B. van Merrienboer, D. Bahdanau, and Y. Bengio, "On the properties of neural machine translation: Encoder-decoder approaches," in *Proc. SSST-8, 8th Workshop Syntax, Semantics Struct. Stat. Transl.*, Doha, Qatar: Association for Computational Linguistics, 2014, pp. 103–111, doi: 10.3115/v1/W14-4012.

[28] G. A. Busari and D. H. Lim, "Crude oil price prediction: A comparison between AdaBoost-LSTM and AdaBoost-GRU for improving forecasting performance," *Comput. Chem. Eng.*, vol. 155, Dec. 2021, Art. no. 107513, doi: 10.1016/j.compchemeng.2021.107513.

[29] I. A. L. Magalhaes et al., "Comparing machine and deep learning methods for the phenology-based classification of land cover types in the Amazon biome using Sentinel-1 time series," *Remote Sens.*, vol. 14, no. 19, Oct. 2022, Art. no. 4858, doi: 10.3390/rs14194858.

[30] L. Bi, G. Hu, M. M. Raza, Y. Kandel, L. Leandro, and D. Mueller, "A gated recurrent units (GRU)-based model for early detection of soybean sudden death syndrome through time-series satellite imagery," *Remote Sens.*, vol. 12, no. 21, Jan. 2020, Art. no. 3621, doi: 10.3390/rs12213621.

[31] P. Zhang et al., "Simulation model of vegetation dynamics by combining static and dynamic data using the gated recurrent unit neural network-based method," *Int. J. Appl. Earth Observ. Geoinf.*, vol. 112, Aug. 2022, Art. no. 102901, doi: 10.1016/j.jag.2022.102901.

[32] P. Guan, L. Zhu, and Y. Zheng, "A study of forest phenology prediction based on GRU models," *Appl. Sci.*, vol. 13, no. 8, Jan. 2023, Art. no. 4898, doi: 10.3390/app13084898.

[33] Z. Niu et al., "Recurrent attention unit: A new gated recurrent unit for long-term memory of important parts in sequential data," *Neurocomputing*, vol. 517, pp. 1–9, Jan. 2023, doi: 10.1016/j.neucom.2022.10.050.

[34] Planet Labs Inc., "Planet | homepage," Planet, Accessed: Jul. 24, 2023. [Online]. Available: https://www.planet.com/

[35] Planet, "Planet imagery product specifications," May 2022. Accessed: Jul. 24, 2023. [Online]. Available: https://assets.planet.com/docs/Planet_Combined_Imagery_Product_Specs_letter_screen.pdf

[36] Sentinel Hub, "Sentinel hub," Accessed: Aug. 07, 2023. [Online]. Available: https://www.sentinel-hub.com/

[37] MKGP, "MKGP - portal," Accessed: Jan. 25, 2023. [Online]. Available: https://rkg.gov.si/vstop/

[38] A. Savitzky and M. J. E. Golay, "Smoothing and differentiation of data by simplified least squares procedures," *Anal. Chem.*, vol. 36, no. 8, pp. 1627–1639, Jul. 1964, doi: 10.1021/ac60214a047.

[39] J. Chung, C. Gulcehre, K. Cho, and Y. Bengio, "Empirical evaluation of gated recurrent neural networks on sequence modeling," in *Proc. NIPS Workshop Deep Learn.*, Dec. 2014, doi: 10.48550/arXiv.1412.3555.

[40] L. Breiman, "Random forests," *Mach. Learn.*, vol. 45, no. 1, pp. 5–32, Oct. 2001, doi: 10.1023/A:1010933404324.

[41] G. E. P. Box, G. M. Jenkins, G. C. Reinsel, and G. M. Ljung, *Time Series Analysis: Forecasting and Control*. Hoboken, NJ, USA: Wiley, 2015.

[42] L. Mou and X. X. Zhu, "A recurrent convolutional neural network for land cover change detection in multispectral images," in *Proc. Int.*

Geosci. Remote Sens. Symp. IEEE Int. Geosci. Remote Sens. Symp., 2018, pp. 4363–4366, doi: 10.1109/IGARSS.2018.8517375.

[43] M. M. Najafabadi, F. Villanustre, T. M. Khoshgoftaar, N. Seliya, R. Wald, and E. Muharemagic, "Deep learning applications and challenges in big data analytics," *J. Big Data*, vol. 2, no. 1, pp. 1–21, Feb. 2015, doi: 10.1186/s40537-014-0007-7.

[44] M. G. Ziliani et al., "Early season prediction of within-field crop yield variability by assimilating CubeSat data into a crop model," *Agricultural Forest Meteorol.*, vol. 313, Feb. 2022, Art. no. 108736, doi: 10.1016/j.agrformet.2021.108736.

Aleš Marsetič received the B.S. degree in geodetic engineering and the Ph.D. degree in geodetic sciences from the University of Ljubljana, Ljubljana, Slovenia, in 2005 and 2015, respectively.

Since 2006, he has been a Research Fellow with the Research Centre of the Slovenian Academy of Sciences and Arts, Ljubljana, Slovenia. From 2010, he is also with the Department of Remote Sensing, the Centre of Excellence for Space Sciences and Technologies (Space-SI). He has authored one book and more than 40 scientific papers. His main research interests include photogrammetric applications in satellite remote sensing. Besides photogrammetry (orthorectification, DSM generation), his field of work also encompasses optical satellite imagery registration and processing, and machine learning algorithms for classification and prediction. He has expertise in the automatization of satellite data preprocessing and in the designing of small satellites and development of their ground segment data processing algorithms.

Dr. Marsetič was the recipient of the 3rd Mission Idea Contest for Micro and Nano-Satellites Utilization First Place Award in 2014, and the Research Centre of the Slovenian Academy of Sciences and Arts Silver Award, in 2016.

Urška Kanjir received the B.S. degree in geodetic engineering and the Ph.D. degree in environmental protection from the University of Ljubljana (UL), Ljubljana, Slovenia, in 2009 and 2021, respectively.

Since 2010, she has been working with the Department of Remote Sensing, the Research Centre of the Slovenian Academy of Sciences and Arts, Ljubljana, Slovenia. She has also worked for the Center of Excellence for Space, Science and Technology (Space-SI) and Faculty of Arts (UL). She has authored more than 40 scientific papers and has participated in many international and national research or application projects dealing with various topics over the years. In her work, she often collaborates with colleagues from other disciplines, especially anthropologists.

Dr. Kanjir was the recipient of the Recognition of Excellence in Service to International Society for Photogrammetry and Remote Sensing, in 2016.